Journal of Materials Chemistry C

COMMUNICATION

View Article Online
View Journal | View Issue

Cite this: J. Mater. Chem. C, 2015, 3, 1468

Received 2nd September 2014
Accepted 22nd December 2014

DOI: 10.1039/c4tc01969e

www.rsc.org/MaterialsC

Charge transport in nanoparticular thin films of zinc oxide and aluminum-doped zinc oxide†

Thomas Lenz,‡[a] Moses Richter,[a] Gebhard J. Matt,*[a] Norman A. Luechinger,[b] Samuel C. Halim,[b] Wolfgang Heiss[c] and Christoph J. Brabec[a]

In this work, we report on the electrical characterization of nanoparticular thin films of zinc oxide (ZnO) and aluminum-doped ZnO (AZO). Temperature-dependent current–voltage measurements revealed that charge transport for both, ZnO and AZO, is well described by the Poole–Frenkel model and excellent agreement between the experimental data and the theoretical predictions is demonstrated. For the first time it is shown that the nature of the charge-transport is not affected by the doping of the nanoparticles and it is proposed that the Poole–Frenkel effect is an intrinsic and universally limiting mechanism for the charge transport in nanoparticular thin films with defect states within the bandgap.

Zinc oxide (ZnO) – a II–VI compound semiconductor with a large band gap (3.37 eV)[1] – exhibits an excitingly widespread range of potential applications,[2] such as lasers,[1] field-effect transistors,[3–5] transducers,[6] varistors,[7] sensors,[8] UV-detectors[9] and also thin-film solar cells, where it can serve as an active[10,11] or interfacial[12,13] or electrode material.[14]

Moreover, ZnO is a promising material in the field of transparent[3,4,15] and flexible electronics,[15,16] because large-area solution processing on flexible substrates using techniques like inkjet printing appears feasible.[17,18] The solutions for film deposition are either based on the sol–gel route or on nanoparticle synthesis. The latter has the advantage that the synthesis and the film deposition can be separated from each other. As pointed out previously,[19,20] this allows cheap and high-throughput synthesis at elevated temperatures, while the film deposition is achieved at lower temperatures, which is a prerequisite for the use of flexible (often polymer-based) substrates.

The problem of nanoparticulate ZnO thin films deposited at low temperatures is that they hardly reach the electric performance of zinc oxide films based on sputtering[21] or spray pyrolysis.[22] Therefore, a better understanding of the electric conduction in these films is desired.

So far, most of the charge transport studies on ZnO nanoparticle films used the transistor device structure: Meulenkamp[23] and Roest *et al.*[24,25] studied ZnO nanoparticles with small sizes (≈5 nm) permeated in electrolyte solutions and it was demonstrated that transport occurs *via* tunnelling between discrete electronic states with or without additional thermal activation depending on the characteristics of the electrolyte.[25] Besides, space-charge limited conduction (SCLC) was shown for ZnO by Bubel *et al.*[19] and by Caglar *et al.*[26] (sandwich device geometry). In these two cases,[19,26] the sizes of the nanostructures were larger (above 25 nm) compared to the above-mentioned reports. This might partially explain the different findings.

Discrepancies between various transport investigations were also revealed for other nanoparticular materials, *e.g.* for nanostructured films of silicon. Besides hopping,[27,28] SCLC,[29] the Poole–Frenkel effect,[30,31] and tunnelling[32,33] were reported for nano-Si (porous silicon or nanoparticles). These inconsistent results further emphasize the need for a detailed description of charge transport in nanoparticular films.

In this work, the charge transport of nanoparticulate ZnO and AZO thin films was investigated. A dispersion of ligand-stabilized ZnO or AZO nanoparticles was deposited on top of an ITO substrate *via* multiple doctor blading[34,35] steps. The resulting film thickness is 0.7–1 μm. Afterwards the sample was transferred to a vacuum chamber equipped with a physical vapor deposition (PVD) system for deposition of a 100 nm thick Ag top contact (for further details see ESI†).

[a]Institute Materials for Electronic and Energy Technology (i-MEET), Department of Materials Science, Friedrich-Alexander-Universität (FAU), Martensstraße 7, 91058, Germany. E-mail: gebhard.matt@ww.uni-erlangen.de; Fax: +49 9131 8528495; Tel: +49 9131 8527726

[b]Nanograde Ltd, Staefa, Laubisrütistr. 50, CH-8712, Switzerland

[c]Institute for Solid-State and Semiconductor Physics, Johannes Kepler University, Linz, Austria

† Electronic supplementary information (ESI) available: The experimental procedure, the symmetry of the *J–V* data of AZO and ZnO, the fitting of the AZO *J–V* plot and tables containing the data related to Fig. 2b and 3b. See DOI: 10.1039/c4tc01969e

‡ Current address: Max-Planck-Institute for Polymer Research, Ackermannweg 10, 55128 Mainz, Germany.

The commercially available ZnO/AZO dispersions from Nanograde Ltd were selected for the investigations. These nanoparticles were produced by flame spray synthesis[36–38] and are expected to have high crystallinity and no adverse surface ligands. In a flame spray synthesis a precursor solution of Zn-acetate is fed (5 ml min^{-1}) to a spray nozzle, dispersed by oxygen (7 l min^{-1}) and ignited by a premixed methane–oxygen flame (CH_4: 1.2 l min^{-1}, O_2: 2.2 l min^{-1}). For the synthesis of AZO nanoparticles with a nominal composition of 2 wt% Al_2O_3 in ZnO, the same Zn-acetate precursor with additional Al-acetylacetonate 2-ethylhexanoic acid under the same process conditions was used. The nanoparticles were collected by air-filtration of the off-gas. In order to prepare stable suspensions of ZnO/AZO, 5 wt% of nanoparticles were dispersed in ethanol by the use of a phosphonate-based ligand.

The ZnO/AZO nanoparticles are crystalline with a diameter of 10–15 nm (see Fig. 1). Due to the high temperatures within the flame spray synthesis and the precisely controlled process conditions, the nanoparticles exhibit high purity and controlled stoichiometric correlation between the dopant material and the oxides.

Fig. 2a and 3a depict the current density–voltage (*J*–*V*) characteristics for AZO (thickness of 950 nm) and ZnO (740 nm), respectively, at various temperatures. The *J*–*V* characteristics appear to be symmetric (within 5%) with respect to the bias (see Fig. S1†). We tested different models to fit the *J*–*V* data of both materials. Consistent and precise results could only be obtained with a combination of Ohm's law for low voltages and the Poole–Frenkel (PF) effect for higher voltages (see Fig. S2†). The former is not unexpected, as Ohm's law is usually valid for the low-voltage – intrinsic – regime of a low-conductivity material.[39] In contrast, the occurrence of the PF effect[40–42] is rather surprising, as it was originally derived for band-like insulators,

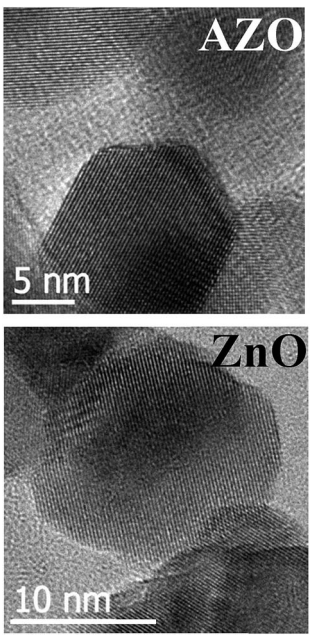

Fig. 1 Transmission electron microscopy images for AZO and ZnO nanoparticles.

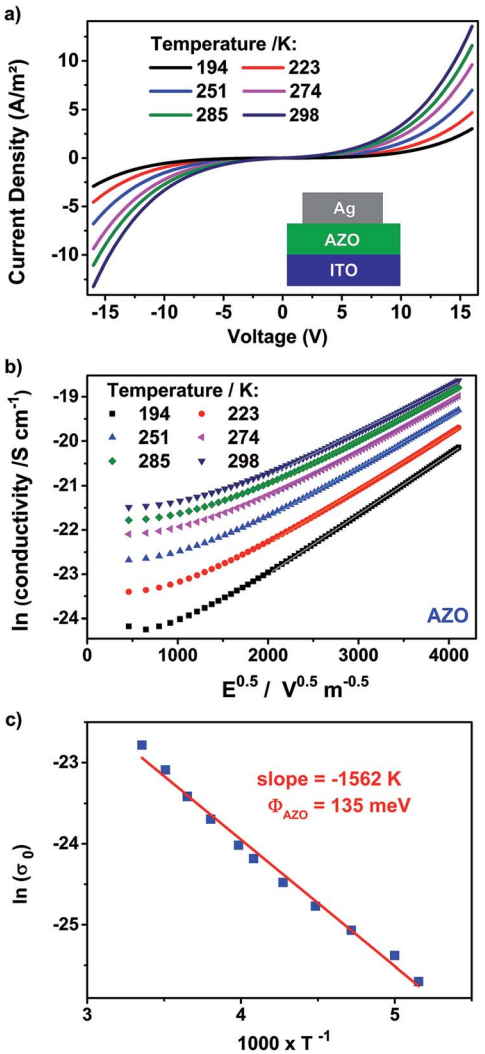

Fig. 2 (a) Current density–voltage (*J*–*V*) characteristics of AZO (950 nm) recorded at different temperatures. The inset shows the device setup. (b) Natural logarithm of conductivity determined for the *J*–*V* data of AZO *versus* the square root of the applied electric field. This plot corresponds to eqn (3). (c) The *y*-intercepts of the linear fit functions ($\ln\sigma_0$) in (b) are plotted *versus* the inverse of temperature to determine the trap barrier height.

such as Si_3O_4 (ref. 43) or Ta_2O_5,[44] which contain traps limiting conductivity. The PF effect describes the lowering of the trap barrier height Φ due to an external electric field E and conductivity σ as follows:[40–42]

$$\sigma = \sigma_{\text{const}} \exp\left(\frac{\beta\sqrt{E} - \Phi}{kT}\right). \quad (1)$$

Here, σ_{const} is the conductivity constant, k is the Boltzmann constant and T is the absolute temperature. The factor β deserves special attention, because it only depends on fundamental physical constants and the dielectric constant ε_r of the material

$$\beta = \sqrt{\frac{e^3}{\varepsilon_0 \pi \varepsilon_r}}, \quad (2)$$

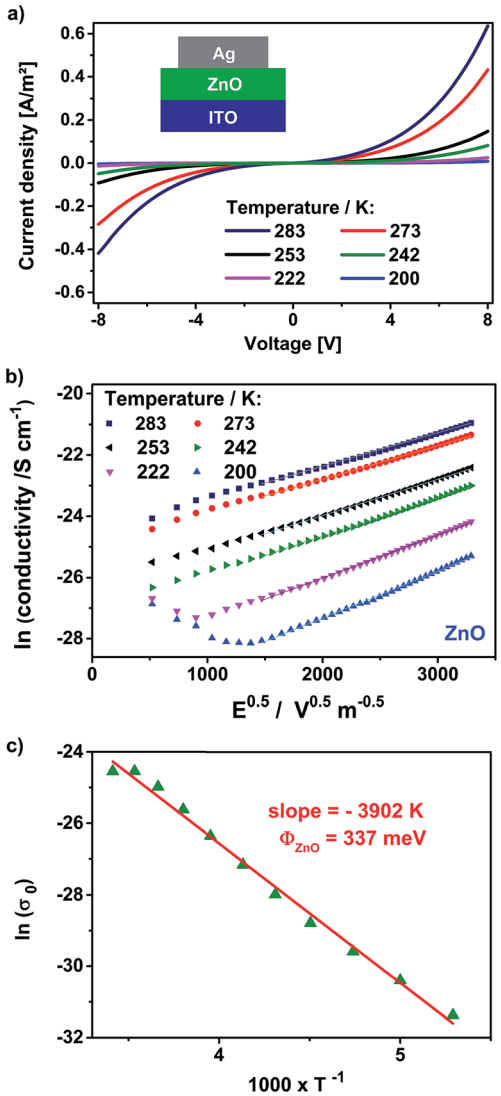

Fig. 3 (a) Current density–voltage (J–V) characteristics of ZnO (740 nm) recorded at different temperatures. The inset shows the device setup. (b) Natural logarithm of conductivity determined for the J–V data of ZnO *versus* the square root of the applied electric field. This plot corresponds to eqn (3). (c) The y-intercepts of the linear fit functions ($\ln\sigma_0$) in (b) are plotted *versus* the inverse of temperature to determine the trap barrier height.

where e is the electronic charge and ε_0 is the permittivity of vacuum.

For the determination of β_{exp} based on the J–V data of ZnO and AZO, we apply the natural logarithm to both sides of eqn (1) leading to

$$\ln(\sigma) = \frac{\beta}{kT}\sqrt{E} + \left\{\ln(\sigma_{const}) - \frac{\Phi}{kT}\right\}. \quad (3)$$

Following eqn (3), Fig. 2b and 3b depict the natural logarithm of conductivity *versus* the square root of the electric field for AZO and ZnO, respectively. Both graphs show broad linear regimes for the datasets for all considered temperatures. The slopes and the y-intercepts of these linear regimes are listed in Tables 1 and 2 in the ESI† together with the resulting values of β.

The experimentally derived values of β_{exp} are *not temperature dependent* with mean values of $\beta_{exp} = 2.64 \pm 0.06 \times 10^{-5}$ eV m$^{0.5}$ V$^{-0.5}$ for ZnO and $\beta_{exp} = 2.42 \pm 0.11 \times 10^{-5}$ eV m$^{0.5}$ V$^{-0.5}$ for AZO. This is in extraordinarily good accordance with the theoretical values of $\beta_{theo} = 2.57 \times 10^{-5}$ eV m$^{0.5}$ V$^{-0.5}$ based on $\varepsilon_r = 8.72$ for ZnO and of $\beta_{theo} = 2.43 \times 10^{-5}$ eV m$^{0.5}$ V$^{-0.5}$ based on $\varepsilon_r = 9.72$ for AZO. The respective dielectric constants were measured with an independent impedance measurement and are confirmed by results from the literature.[45]

We emphasize that our results are in stark contrast to comparable transport studies investigating the PF effect in nanostructured silicon.[30,31] In those reports, the experimentally and theoretically derived values of ε_r, which directly correlate with β, were completely different. It was argued that the theory behind the PF effect might not be adaptable to nanostructured films, because these films would not provide a straight-forward physical meaning of ε_r. Here, we show that β_{exp} and β_{theo} can indeed match remarkably and thus unambiguously prove the PF effect. We note that the values of β_{exp} at lower temperatures show a larger deviation from β_{theo} for AZO, but the plot of $\ln(\sigma)$ *versus* $\sqrt{E}$ still provides broad linear regimes particularly for higher voltages. This rules out other transport mechanisms, such as tunneling or SCLC.[46] Another possibility which should also be considered is Richardson–Schottky emission: it is the attenuation of a metal–insulator barrier arising from electrode image–force interaction with the field at the metal–insulator interface.[47] The Richardson–Schottky (RS) effect and the PF effect are easily mixed up, as the J–V characteristics follow the same functional dependency on the electric field but the exponent for the RS effect is by a factor of 2 smaller. Therefore, our results clearly underline that transport in nanoparticular ZnO and AZO follows the PF theory and not the RS theory. Moreover, the symmetry of the J–V characteristics despite the asymmetric contacts and the film thickness in the micrometre range clearly demonstrate that the conduction through the sandwich devices is bulk-limited (Poole–Frenkel), and not electrode-limited (Richardson–Schottky).

We sought to determine the barrier height Φ for AZO and ZnO. From eqn (1) it is evident that the conductivity at zero electric field (σ_0) is thermally activated. Fig. 2c and 3c show an Arrhenius plot of (σ_0) for ZnO and AZO. Note that $\ln(\sigma_0)$ equals the y-intercept of the linear regimes in Fig. 2b and 3b. The activation energies determined from the slopes in Fig. 2c and 3c are $\Phi_{AZO} = 135$ meV and $\Phi_{ZnO} = 337$ meV, respectively.

We emphasize that the activation energy of ZnO is by more than a factor of 2 higher than that of AZO but β_{exp} is practically the same for AZO and ZnO. This suggests that the nature of the charge transport mechanism is *equivalent* for intrinsic ZnO and AZO.

The question arises why electron transport through these nanoparticular thin films is so well described by the PF theory.

Due to the low post-deposition temperature, the thin films of AZO/ZnO can be considered as 3D assemblies of single nanoparticles (neck formation between neighboring nanoparticles is not expected at 80 °C).[23] Electron conduction across the film

requires that electrons are transferred from one nanoparticle to its next neighbor and so forth.

Practically such a hopping transport at higher temperatures is very likely to be thermally activated following $\sigma \propto \exp\left(\frac{-\Delta E}{T}\right)$. It is noted that a more complex temperature dependency is typically just observed in the limit of low temperatures and/or in amorphous systems.[48,49]

On the other hand, the electric field often strongly influences charge transport in such systems.[50,51] However, to the best of the authors' knowledge, this is the first time that Poole–Frenkel-like charge transport was found in nanoparticulate thin films.

In order to experience the PF effect, a trap is required to be positively *charged when empty* and *uncharged when filled*.[41] Consequently, the interaction between the positively charged trap and the trapped electron gives rise to a coulombic barrier. The question remains what the origin of the observed activation energies in AZO ($\Phi_{AZO} = 135$ meV) and ZnO ($\Phi_{ZnO} = 337$ meV) is.

In the literature, defects in ZnO (single crystal or sputtered film) with similar energy values have been observed in DLTS and impedance spectroscopy.[52–56] Ref. 53 suggests that these defects might relate to the incorporation of oxygen in the crystal lattice. We emphasize that the origin of defects in ZnO is generally under debate in the literature[52–58] and that a direct comparison with the literature needs to be done with caution, as the defect density is sensitively affected by the growth method and annealing conditions. In addition, the flame spray synthesis utilized in this work is a new and novel production method.

The lower observed activation energy for the AZO thin films is due to the higher free electron concentration. Al is a shallow donor in ZnO (in ref. 59, it was shown that Al is even substitutionally shallow) and by the increased free charge-carrier concentration the Fermi-energy is closer to the "transport-band". Consequently the thermal activation energy for the charge transport is reduced. In either case the nature of charge transport remains unaffected by the Al doping and is limited by the inter-particle charge transport. We suggest that this might be attributed to surface defects, which always occur due to unsaturated bonds on the surface, but further investigations are needed to test this hypothesis.

Conclusion

In this work, the conduction through nanoparticulate ZnO and AZO thin films was investigated. While the *J–V* characteristics at low voltage obey Ohm's law, transport in the high voltage data regime is dominated by the Poole–Frenkel effect. It is outlined that the occurrence of the Poole–Frenkel effect is related to coulombically bound electrons, which have to overcome a field-dependent barrier to the next nanoparticle. It is demonstrated that the conduction mechanism is equivalent for the AZO nanoparticles, where Al acts as a shallow donor. To the best of our knowledge, this is the first time that the Poole–Frenkel effect was unambiguously demonstrated as the dominant transport mechanism in a nanoparticulate thin film.

Acknowledgements

This work has been partially funded by the Sonderforschungsbereich 953 "Synthetic Carbon Allotropes" (DFG) and the Gradko 1896 "*in situ* Microscopy" (DFG). We also thank the support of Solar Technologies go Hybrid (SolTech) project. Moreover, we would like to thank Wolfgang Grafeneder and Ronald Wirth for technical support.

References

1 M. H. Huang, S. Mao, H. Feick, H. Yan, Y. Wu, H. Kind, E. Weber, R. Russo and P. Yang, *Science*, 2001, **292**(5523), 1897–1899.
2 Ü. Özgür, Y. I. Alivov, C. Liu, A. Teke, M. A. Reshchikov, S. Doğan, V. Avrutin, S. J. Cho and H. Morkoç, *J. Appl. Phys.*, 2005, **98**(4), 1–103.
3 R. L. Hoffman, B. J. Norris and J. F. Wager, *Appl. Phys. Lett.*, 2003, **82**(5), 733–735.
4 E. Fortunato, P. Barquinha, A. Pimentel, A. Gonçalves, A. Marques, L. Pereira and R. Martins, *Thin Solid Films*, 2005, **487**(1–2), 205–211.
5 E. M. C. Fortunato, P. M. C. Barquinha, A. C. M. B. G. Pimentel, A. M. F. Gonçalves, A. J. S. Marques, L. M. N. Pereira and R. F. P. Martins, *Adv. Mater.*, 2005, **17**(5), 590–594.
6 P. M. Martin, M. S. Good, J. W. Johnston, G. J. Posakony, L. J. Bond and S. L. Crawford, *Thin Solid Films*, 2000, **379**(1–2), 253–258.
7 K. Mukae, K. Tsuda and I. Nagasawa, *J. Appl. Phys.*, 1979, **50**(6), 4475–4476.
8 P. Mitra, A. P. Chatterjee and H. S. Maiti, *Mater. Lett.*, 1998, **35**(1–2), 33–38.
9 Y. Jin, J. Wang, B. Sun, J. C. Blakesley and N. C. Greenham, *Nano Lett.*, 2008, **8**(6), 1649–1653.
10 W. J. E. Beek, M. M. Wienk and R. A. J. Janssen, *Adv. Funct. Mater.*, 2006, **16**(8), 1112–1116.
11 P. Ravirajan, A. M. Peiró, M. K. Nazeeruddin, M. Graetzel, D. D. C. Bradley, J. R. Durrant and J. Nelson, *J. Phys. Chem. B*, 2006, **110**(15), 7635–7639.
12 T. Stubhan; I. Litzov; N. Li; H. Q. Wang; J. Krantz; F. MacHui; M. Steidl; H. Oh; G. J. Matt; C. J. Brabec In *Low temperature, solution processed metal oxide buffer layers fulfilling large area production requirements*, 2012.
13 J. Gilot, M. M. Wienk and R. A. J. Janssen, *Appl. Phys. Lett.*, 2007, **90**(14), 143512.
14 K. Ramanathan, M. A. Contreras, C. L. Perkins, S. Asher, F. S. Hasoon, J. Keane, D. Young, M. Romero, W. Metzger, R. Noufi, J. Ward and A. Duda, *Prog. Photovoltaics*, 2003, **11**(4), 225–230.
15 C. Y. Lee, M. Y. Lin, W. H. Wu, J. Y. Wang, Y. Chou, W. F. Su, Y. F. Chen and C. F. Lin, *Semicond. Sci. Technol.*, 2010, **25**(10), 105008.
16 L. W. Ji, C. Z. Wu, T. H. Fang, Y. J. Hsiao, T. H. Meen, W. Water, Z. W. Chiu and K. T. Lam, *IEEE Sens. J.*, 2013, **13**(12), 4940–4943.
17 Y. Y. Noh, X. Cheng, H. Sirringhaus, J. I. Sohn, M. E. Welland and D. J. Kang, *Appl. Phys. Lett.*, 2007, **91**(4), 043109.

18 T. V. Richter, F. Stelzl, J. Schulz-Gericke, B. Kerscher, U. Würfel, M. Niggemann and S. Ludwigs, *J. Mater. Chem.*, 2010, **20**(5), 874–879.
19 S. Bubel, N. Mechau, H. Hahn and R. Schmechel, *J. Appl. Phys.*, 2010, **108**(12), 124502.
20 D. Weber, S. Botnaraş, D. V. Pham, J. Steiger and L. De Cola, *J. Mater. Chem. C*, 2013, **1**(18), 3098–3101.
21 T. Minami, H. Nanto and S. Takata, *Appl. Phys. Lett.*, 1982, **41**(10), 958–960.
22 A. Bashir, P. H. Wöbkenberg, J. Smith, J. M. Ball, G. Adamopoulos, D. D. C. Bradley and T. D. Anthopoulos, *Adv. Mater.*, 2009, **21**(21), 2226–2231.
23 E. A. Meulenkamp, *J. Phys. Chem. B*, 1999, **103**(37), 7831–7838.
24 A. L. Roest, A. Germeau, J. J. Kelly, D. Vanmaekelbergh, G. Allan and E. A. Meulenkamp, *ChemPhysChem*, 2003, **4**(9), 959–966.
25 A. L. Roest, J. J. Kelly and D. Vanmaekelbergh, *Appl. Phys. Lett.*, 2003, **83**(26), 5530–5532.
26 Y. Caglar, M. Caglar, S. Ilican and F. Yakuphanoglu, *Phys. B*, 2007, **392**(1–2), 99–103.
27 M. Ben-Chorin, F. Möller, F. Koch, W. Schirmacher and M. Eberhard, *Phys. Rev. B: Condens. Matter Mater. Phys.*, 1995, **51**(4), 2199–2213.
28 M. A. Rafiq, Y. Tsuchiya, H. Mizuta, S. Oda, S. Uno, Z. A. K. Durrani and W. I. Milne, *J. Appl. Phys.*, 2006, **100**(1), 014303.
29 C. Peng, K. D. Hirschman and P. M. Fauchet, *J. Appl. Phys.*, 1996, **80**(1), 295–300.
30 M. Ben-Chorin, F. Möller and F. Koch, *Phys. Rev. B: Condens. Matter Mater. Phys.*, 1994, **49**(4), 2981–2984.
31 X. Zhou, K. Uchida, H. Mizuta and S. Oda, *J. Appl. Phys.*, 2009, **105**(12), 124518.
32 T. A. Burr, A. A. Seraphin, E. Werwa and K. D. Kolenbrander, *Phys. Rev. B: Condens. Matter Mater. Phys.*, 1997, **56**(8), 4818–4824.
33 L. Tsybeskov, S. P. Duttagupta, K. D. Hirschman and P. M. Fauchet, *Appl. Phys. Lett.*, 1996, **68**(15), 2058–2060.
34 N. Li, D. Baran, K. Forberich, F. Machui, T. Ameri, M. Turbiez, M. Carrasco-Orozco, M. Drees, A. Facchetti, F. C. Krebs and C. J. Brabec, *Energy Environ. Sci.*, 2013, **6**(12), 3407–3413.
35 T. Stubhan, H. Oh, L. Pinna, J. Krantz, I. Litzov and C. J. Brabec, *Org. Electron.*, 2011, **12**(9), 1539–1543.
36 W. J. Stark, K. Wegner, S. E. Pratsinis and A. Baiker, *J. Catal.*, 2001, **197**(1), 182–191.
37 E. K. Athanassiou, R. N. Grass and W. J. Stark, *Nanotechnology*, 2006, **17**(6), 1668.
38 S. Loher, W. J. Stark, M. Maciejewski, A. Baiker, S. E. Pratsinis, D. Reichardt, F. Maspero, F. Krumeich and D. Günther, *Chem. Mater.*, 2004, **17**(1), 36–42.
39 M. A. Lampert and P. Mark, *Current Injection in Solids*, Academic Press, New York, 1970.
40 J. Frenkel, *Phys. Rev.*, 1938, **54**(8), 647–648.
41 J. G. Simmons, *Phys. Rev.*, 1967, **155**(3), 657–660.
42 J. G. Simmons, *J. Phys. D: Appl. Phys.*, 1971, **4**(5), 613–657.
43 S. M. Sze, *J. Appl. Phys.*, 1967, **38**(7), 2951–2956.
44 C. A. Mead, *Phys. Rev.*, 1962, **128**(5), 2088–2093.
45 M. Shim and P. Guyot-Sionnest, *J. Am. Chem. Soc.*, 2001, **123**(47), 11651–11654.
46 A. K. Jonscher, *Thin Solid Films*, 1967, **1**(3), 213–234.
47 S. Sze and K. K. Ng, *Physics of Semiconductor Devices*, Third edn, 2006, pp. 1–815.
48 N. F. Mott, *Philos. Mag.*, 1969, **19**(160), 835–852.
49 H. Bässler, *Phys. Status Solidi B*, 1993, **175**(1), 15–56.
50 D. M. Pai, *J. Chem. Phys.*, 1970, **52**(5), 2285–2291.
51 H. C. F. Martens, P. W. M. Blom and H. F. M. Schoo, *Phys. Rev. B: Condens. Matter Mater. Phys.*, 2000, **61**(11), 7489–7493.
52 W. Mtangi, M. Schmidt, F. D. Auret, W. E. Meyer, P. J. Janse Van Rensburg, M. Diale, J. M. Nel, A. G. M. Das, F. C. C. Ling and A. Chawanda, *J. Appl. Phys.*, 2013, **113**(12), 124502.
53 F. D. Auret, W. E. Meyer, P. J. Janse van Rensburg, M. Hayes, J. M. Nel, H. von Wenckstern, H. Schmidt, G. Biehne, H. Hochmuth, M. Lorenz and M. Grundmann, *Phys. B*, 2007, **401–402**, 378–381.
54 F. Schmidt, S. Müller, H. Von Wenckstern, C. P. Dietrich, R. Heinhold, H. S. Kim, M. W. Allen and M. Grundmann, *Appl. Phys. Lett.*, 2013, **103**(6), 062102.
55 J. Bollmann and D. K. Simon, *Phys. B*, 2014, **439**, 14–19.
56 H. Von Wenckstern, H. Schmidt, M. Grundmann, M. W. Allen, P. Miller, R. J. Reeves and S. M. Durbin, *Appl. Phys. Lett.*, 2007, **91**(2), 022913.
57 D. Zhang, J. Zhang, Z. Guo and X. Miao, *J. Alloys Compd.*, 2011, **509**, 5962–5968.
58 D. Zhang, J. Zhang, Y. Cheng, L. Yuan and X. Miao, *J. Am. Ceram. Soc.*, 2010, **93**, 3291–3298.
59 S. B. Orlinskii, J. Schmidt, P. G. Baranov, V. Lorrmann, I. Riedel, D. Rauh and V. Dyakonov, *Phys. Rev. B: Condens. Matter Mater. Phys.*, 2008, **77**(11), 115334.

